11th World Congress on Computational Mechanics (WCCM XI)
5th European Conference on Computational Mechanics (ECCM V)
6th European Conference on Computational Fluid Dynamics (ECFD VI)
E. Oñate, J. Oliver and A. Huerta (Eds)

# WAKE-INTEGRAL METHOD FOR DRAG PREDICTION

**A. CARRE*, M. CORDERO-GRACIA*, M. GÓMEZ* AND J. PONSIN†**

* Escuela Técnica Superior de Ingeniería Aeronáutica y del Espacio (ETSIAE)
Universidad Politécnica de Madrid
Pza. de Cardenal Cisneros, 3, 28040 Madrid, Spain
e-mail: ad.carre@alumnos.upm.es

†Instituto Nacional de Técnica Aeroespacial (INTA)
Carretera Torrejón a Ajalvir, km 4
28850 Torrejón de Ardoz, Madrid, Spain
e-mail: ponsinj@inta.es

**Key words:** Wake Integral, Adaptive Meshing, Drag Extraction

**Abstract.** This paper describes the theoretical development and implementation issues of a far field induced drag extraction tool based on the Maskell integral. Far field methods provide an alternative to classical near field approach, offering the possibility of decompose drag contributions based on their physical source and improves prediction accuracy on coarse meshes. Instead of classical triangulation of intersection nodes contained in the cutting plane, a more regular adaptive mesh is implemented in order to improve flow reconstruction smoothness and accuracy. Both meshes results are compared and the influence of generation parameters of the bidimensional adaptive mesh is discussed. Numerical diffusion plays a major role in vortex decay, and because of that phenomena, a correction factor is needed in order to back as much as possible the cutting plane without loosing precision. Finally, Onera M6 tests are conducted, showing acceptable precision in drag prediction until seven or more chords downstream.

## 1 INTRODUCTION

The successful development of Computational Fluid Dynamics (CFD) methods for solving the Reynolds-averaged Navier-Stokes (RANS) equations has brought the possibility of calculating a complete configuration with resources widely available nowadays. However, drag extraction methods are still developing. Since lift values are typically an order of magnitude higher than drag values, this last one is more difficult to estimate in an accurate and reliable way.

Drag measure has proven to be quite sensitive to grid size and topology, turbulence models or transition estimation [1], [2]. The industry-standard procedure consists on

what is called *near field approach*, where integrals of pressure forces and shear stresses are extended on the surface of the body, obtaining total drag and lift values. Nevertheless, some drawbacks arise from this approach: the obtained measure depends on the surface grid used and drag is obtained as a global quantity, so it is not possible to know each drag contribution separately.

In order to circumvent those problems, a new procedure was developed: the *far field approach*. In opposition to the Near Field Approach, now momentum conservation equation is applied throughout a stream-normal plane located downstream which cuts the body wake. Although the far-field drag prediction approach has been used early in CFD to estimate induced drag in potential codes, in recent years the application of this approach for drag extraction of CFD Navier-Stokes solutions has gained an increasing interest. The reason is that this method allows eliminating spurious drag components generated by numerical and discretisation errors [3], [4] and in addition, drag contributions can be separated based on their physical origin. Another important advantage is that no detailed information of the surface geometry is required at all.

In order to apply this procedure, the cutting plane must be meshed. Most current developments try to recreate the volumetric geometry and remesh resulting convex polygons in triangles. This method requires of small computational effort, but leads to low quality meshes that will affect the solution smoothness and accuracy. In this paper, another approach has been considered: instead of remeshing the resulting cutting plane, a new adaptive quadtree mesh has been implemented. In this way, all the elements will be quadrilateral, that is, profiting from structured mesh solution smoothness. Implementing the quadtree mesh has coupled volumetric and planar meshes, since refinement from the 3D mesh will be inherited by the planar mesh. In addition, user will be capable of strongly controlling minimum and maximum mesh size.

However, this procedure requires an interpolation form cutting plane points to the quadtree mesh nodes. Since the number of cutting plane points can be arbitrarily high, special care should be taken when choosing the interpolation scheme to be used.

This paper will discuss the implementation and results obtained from an Euler subsonic Onera M6 wing solved for two different unstructured meshes, a basic one and a wake-refined one. It will be organised in the following way: section 2 gives an overview of far field drag extraction method, section 3 goes into detail about the two drag contribution integrals that are used in far field methods. From this point on, cases are presented in section 4 and cutting plane meshing strategy is exposed in section 5. Section 6 is dedicated to Maskell correction for Euler flows and section 7 contains the conclusions.

## 2 DRAG DECOMPOSITION

One of the most interesting aspects for far field drag extraction is the capacity of decomposing drag on the basis of the physical phenomena that causes it. According to this philosophy, we find two main formulations in the literature, the so called mid field approach [4], [3] which decompose the far field drag in volume integrals over the zones which

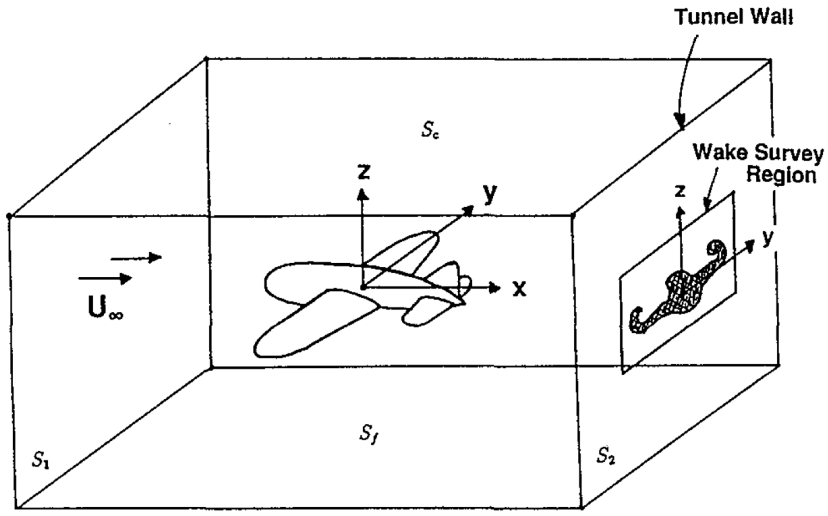


Figure 1: Control volume as defined by Kusunose, extracted from [5]

physically produce drag (boundary layers, shear layers and shock waves) and the wake plane integration approach [5], [6], [7] in which the drag is evaluated through integrals on the wake plane. This last approach, which has been adopted, is more closely related with the classical far-field drag formulae (e.g. induced drag on the Treftz plane). One of the drawbacks of the wake plane approach for drag prediction is the drag transferring between different components as the wake integration plane is located far downstream. Particularly, the predicted induced (vortex) drag decreases due to the numerical dissipation of the trailing tip vortices and the entropy (profile) drag increases for the same reason [2]. In this paper we address this problem and propose some numerical improvements in order to evaluate the induced drag through the Maskell integral, $D_{mask}$.

Maskell [8] asserted that induced drag could be calculated from a surface integral over the whole cross section of the control volume (CV) (fig. 1). The complete derivation of the method can be found in [8] and a well explained summary can be consulted in [5].

Summarising that work, total drag, $D$, can be decomposed in three contributions:

$$D = D_s + D_h + D_{mask} \tag{1}$$

where

$$D_s = \iint \left( p_\infty \frac{s}{R} \right) \, \mathrm{d}y \, \mathrm{d}z \tag{2}$$

$$D_h = \iint \left( -\rho_\infty \Delta H \right) \, \mathrm{d}y \, \mathrm{d}z \tag{3}$$

$$D_{mask} = \frac{1}{2} \rho_\infty \iint \psi \zeta \, \mathrm{d}y \, \mathrm{d}z \tag{4}$$

being $s$ entropy, $H$ stagnation enthalpy, $\Psi$ the cross-flow stream function and $\zeta$ the streamwise component of vorticity.

The drag contribution $D_h$ will not be taken in consideration in this analysis, as enthalpy, $H$, remains constant throughout the domain since only non-powered models are considered.

The last integral, $D_{mask}$, accounts for the drag produced by the trailing tip vortex. In real cases, the tip vortices are dissipated by the viscosity of the air but this phenomena takes place over several body lengths. In numerical computations the dissipation of the vortex occurs in much more shorter distances due to the numerical dissipation. This effect is amplified when unstructured grids are used because the size of the cells typically grows faster downstream than with structured ones, and the numerical dissipation scales to a power of the size of the grid. Therefore, a normal practice is to locate the wake plane as close as possible to the wing trailing edge to avoid the vortex dissipation effect. In this case, the cutting plane necessarily intersects the fuselage for wing-body configuration and the possible contribution of fuselage has to be taken into account. To avoid this situation it would be desirable to locate the wake plane as far as possible downstream, at least at the end of the airplane configuration. In addition, it should be noticed that Maskell integral expresses a direct relationship between induced drag and wing-tip vorticity, so it might be considered as a link between this development and classical lifting line theory.

## 3 MASKELL INTEGRAL EVALUATION

In order to evaluate the Maskell drag integral, $\psi$ must be calculated, which implies solving on the cutting plane the vorticity equation:

$$\nabla^2\psi = \frac{\partial^2\psi}{\partial y^2} + \frac{\partial^2\psi}{\partial z^2} = -\zeta \tag{5}$$

with boundary conditions

$$\psi = 0 \tag{6}$$

to be enforced along the intersection of tunnel walls with the cutting plane.

The resulting system of equations can be solved in two different ways. The first, and more obvious way, is to solve Poisson equation with a numerical solver [9], but it has been found that results were too sensitive to the grid size used in the procedure.

To avoid this drawback, Poisson equation can be solved analytically using Green's function method for elliptic PDEs. This procedure will improve the robustness of the calculation, reducing the grid dependency.

Kusunose [5] described this methodology in detail. Taking into account symmetry planes, the cross-flow stream function in each grid node, $j$, is given by the following

expression:

$$\psi_j = -\frac{1}{4\pi}\sum_{\beta}\left\{\Gamma_\beta\left[\log\left((y_j-y_\beta)^2+(z_j-z_\beta)^2\right)-\log\left((y_j+y_\beta)^2+(z_j-z_\beta)^2\right)\right]\right\} \quad (7)$$

where $\beta$ subindex means the whole of the elements of the cutting plane. The element vorticity, $\Gamma_\beta$ is their vorticity, obtained as:

$$\int_C \zeta \; \mathrm{d}y \; \mathrm{d}z = \int_{\partial C} (v \; \mathrm{d}y + w \; \mathrm{d}z) \quad (8)$$

In the present work, equation (8) has been implemented using a first order interpolation. Since maximum size of planar cells can be effectively limited, it is considered that this scheme will be accurate enough.

## 4 TEST CASES

Two unstructured meshes have been analysed for the same configuration: an Onera M6 wing at 3.06 degrees. Mesh 2 (see figure 2b and table 1b) is similar to mesh 1 (figure 2a and table 1a) but the wake zone has been refined in order to more accurately simulate entropy phenomena and reduce artificial dissipation. A hexahedral source which contains the wake area with an extension downstream of two spans has been prescribed. In this area the size of the elements is enforced to be constant (0.05 relative to the span length). In this source area the tetrahedral elements are created almost isotropically with the same size in all directions.

Both cases have been solved with the compressible DLR TAU-CODE for Euler flow in subsonic conditions ($M = 0.2$). Equations discretisation has been carried on by using central differences with a JST artificial dissipation scheme.

| Elements | tri + tetra |
|---|---|
| Number of Nodes | 795425 |
| Number of Elements | 4559374 |

(a) Mesh 1 parameters

| Elements | tri + tetra |
|---|---|
| Number of Nodes | 1036396 |
| Number of Elements | 5968481 |

(b) Mesh 2 parameters

Table 1: Mesh description for both cases

As one can anticipate, mesh definition will have a noticeable impact on the solution quality. In following sections, it will be illustrated that entropy integral is the most mesh sensitive quantity. Both volumetric and planar meshes will influence the values obtained.

## 5 CUTTING PLANE MESHING BASED ON QUADTREE

Quadtrees and octrees have been used for 2D and 3D mesh generators [10], [11]. The quadtree generation algorithm starts by defining the smallest square containing all the

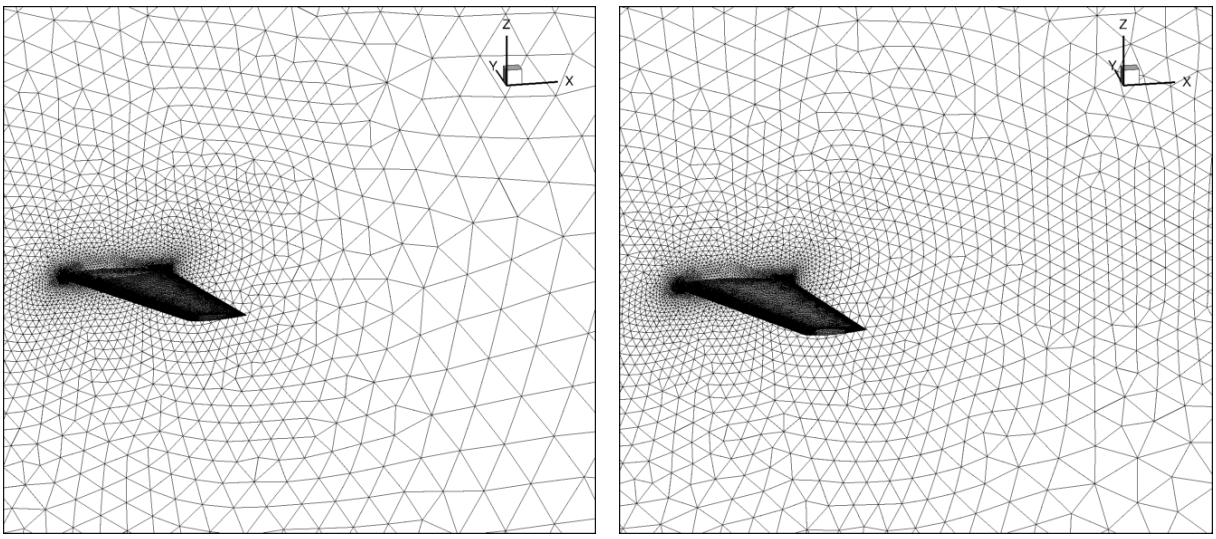


(a) Onera M6 mesh 1 (b) Onera M6 mesh 2

Figure 2: Volumetric meshes used in the analysis

points resulting from the cutting plane. This square is recursively subdivided into four equally-sized children squares, each of which contains at most $N_{max}$ points.

Using the quadtree generation algorithm proposed by Loehner [10] as a staring point, some modifications have been carried on in order to impose a tighter size control over the elements (figure 3) by limiting their minimum level in addition to the $N_{max}$ imposed constraint.

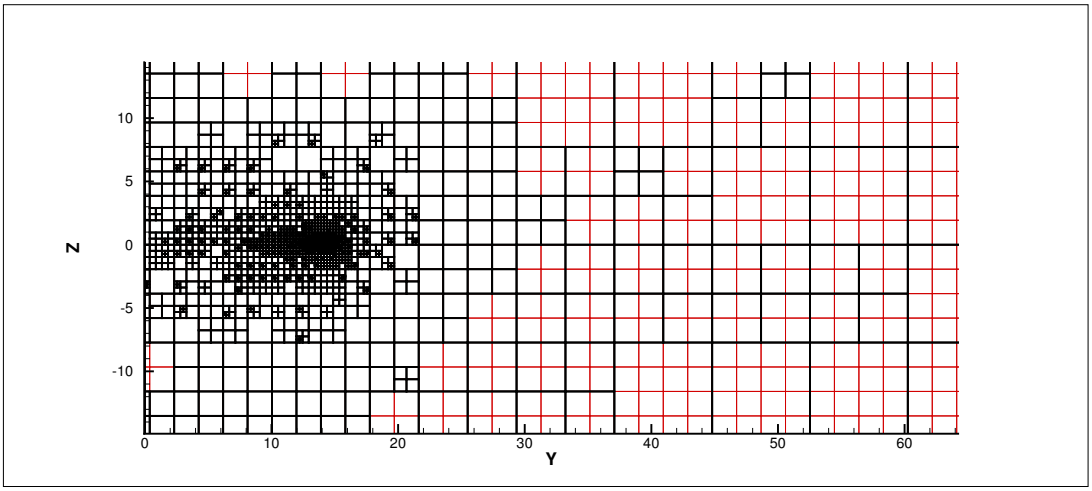


Figure 3: Element maximum size control for quadtree mesh. Red mesh is the refined one.

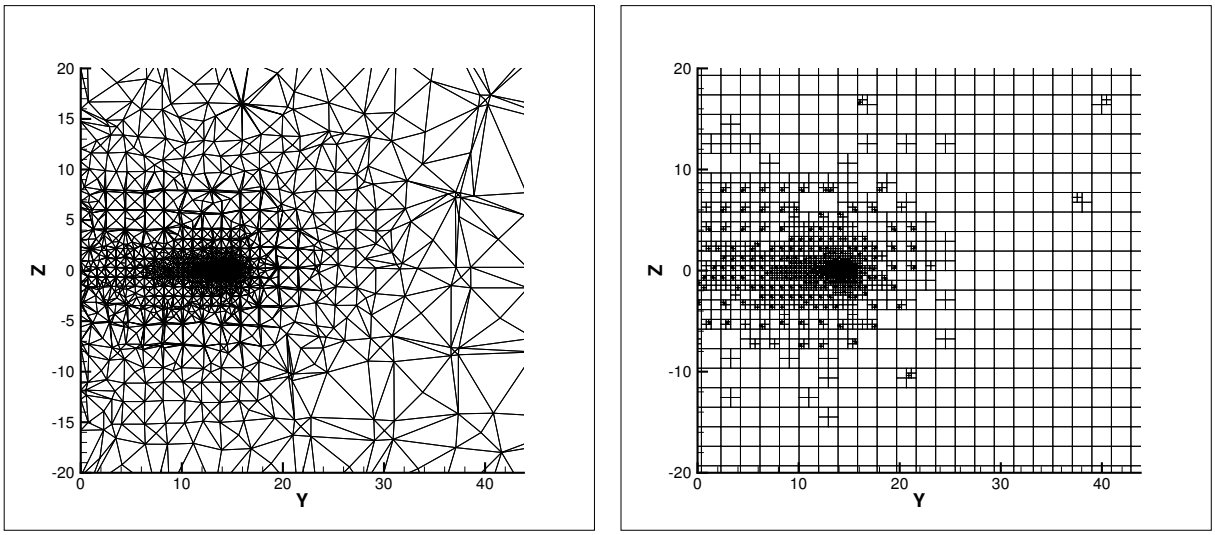


(a) Triangular mesh

(b) New quadtree mesh

Figure 4: Wake zone detail of conventional and adaptive quadtree meshes

Avoiding large elements, interpolation reconstructs in a smoother way small entropy variations that can take place outside the wake, improving the integral (2) accuracy.

Some authors have applied a cut-off filter to the integrals, in order to reduce the integral's domain [2], [12]. We have conducted several tests that have shown that this is for little benefit, with the additional drawback that the cut-off level must be manually adjusted, adding unnecessarily a new degree of freedom which will highly influence the obtained value. For all of this, the integral has been calculated over the whole plane.

In order to evaluate the entropy integral, the points resulting from cutting the mesh with the plane must be meshed. Previous works recreated volumetric geometry and meshed all convex non-triangular resulting elements. In sight of the bad quality of the planar mesh obtained (figure 4a), another approach has been considered. The main requirements that this new mesh must satisfy are:

- Mesh has to be fine enough near the vortex.
- It must be avoided bad quality elements in the wake zone.
- It must be imposed a string control over far field elements size.

In sight of these requirements, quadtree mesh has been implemented with great success (figure 4b). All the elements but the boundaries ones are perfect squares (boundaries are adjusted using rectangles) and the meshing process provides total control over minimum and maximum sizes of the mesh. In addition, adaptive quadtree inherits its refinement from the volumetric mesh, so entropy integral evaluation will benefit from both without having to add any additional degree of freedom in the meshing process. Quadtree

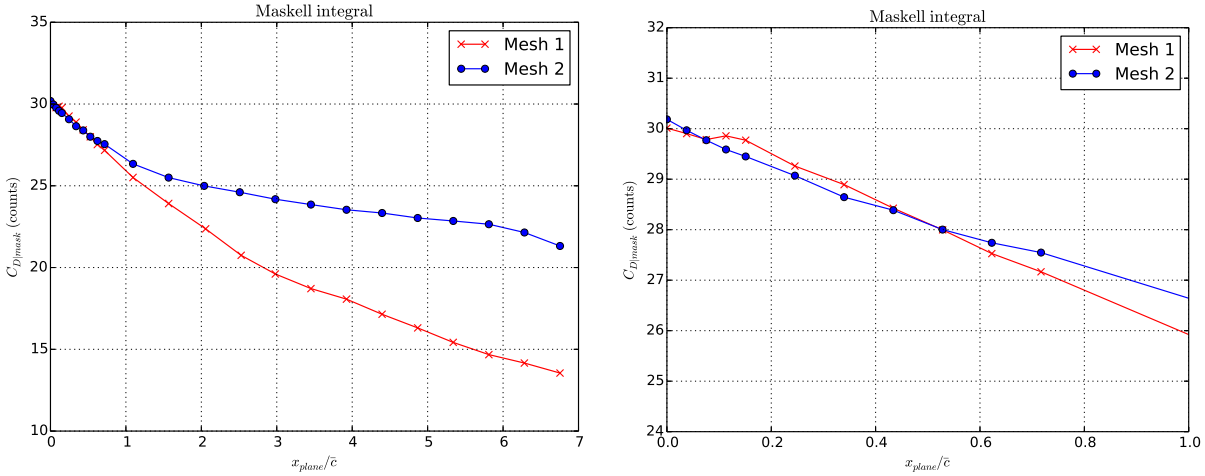


(a) Overall view

(b) 1 chord detail view

Figure 5: Comparison in Maskell integral for the two meshes. Onera M6 at $M = 0.2$ and $\alpha = 3.06°$

mesh will also profit from the fact that it is a near-structured mesh, improving flowfield reconstruction smoothness and accuracy over previous methods.

Several conclusions can be extracted from comparing both of planar meshing processes: adaptive quadtree mesh offers an improvement on integral precision for coarse meshes, but it needs more CPU time because an extra interpolation is needed. Also, tests have shown that Maskell integral (figure 5) has a dependance on the planar mesh used. Values obtained with quadtree meshes show a slightly (over 1-2 counts) greater value than the triangular mesh ones (figure 6).

The presented development has applied a spline interpolation strategy [13] to transfer values from cutting plane points to quadtree mesh nodes. This method has improved wake reconstruction accuracy and smoothness. However, excessively refined wake meshes can result in a higher computational cost due to the linear system that needs to be solved.

## 6 MASKELL CORRECTION FOR EULER FLOWS

Due to numerical dissipation, entropy is generated when vortex are diffused. Because of that lost of vorticity, Maskell integral needs a correction when cutting plane moves downstream (see figure 6).

Since Euler solutions only provide induced drag information for subsonic flows, the entropy integral will be referenced to the first cutting plane, which is located closely behind the wingtip. By considering a sequence of cutting planes, it can be observed that Maskell integral is effectively corrected, the drag measurement staying steady even in cutting planes located further than 5 chords.

Results obtained will depend not only on the mesh, but also on the artificial dissipation

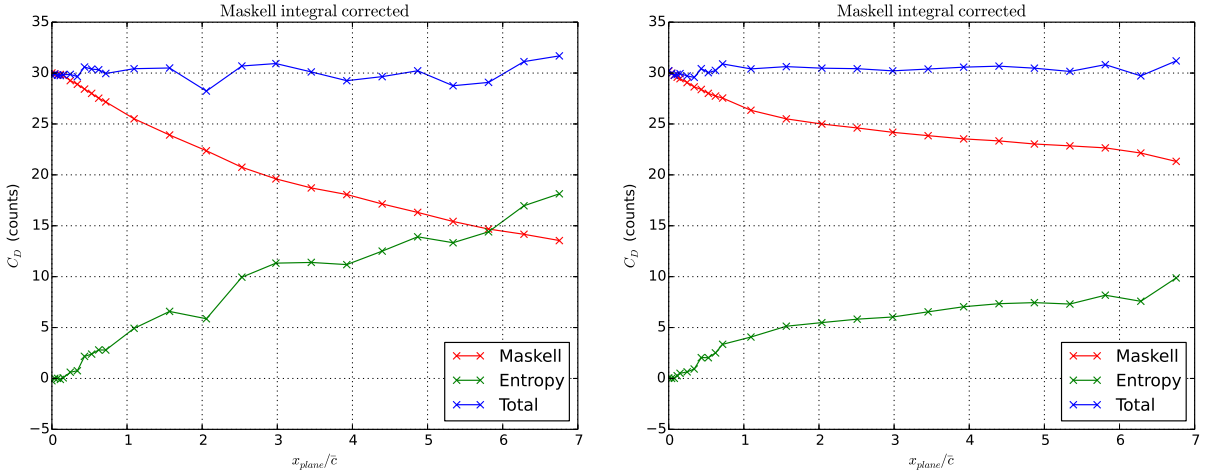


(a) Mesh 1 results

(b) Mesh 2 results

Figure 6: Comparison in corrected Maskell integral for the two meshes. Onera M6 at $M = 0.2$ and $\alpha = 3.06°$

and discretisation scheme applied. All solutions here exposed are solved using a JST artificial dissipation scheme with central differences. More diffusive schemes have been tested, showing that integral can be effectively corrected during a reasonable downstream distance.

As can be seen, volumetric mesh refinement (hence, planar mesh refinement) leads to an improvement of the smoothness of the solution due to the increased accuracy of the entropy integral. Anyway, the average induced drag value remains constant between the two meshes.

## 7 CONCLUSIONS

Wake integral methods have been receiving increasing interest in recent times due to the possibility of eliminating spurious drag generated by numerical sources. Also, induced drag can be evaluated separately from the other contributions, supplying the designers with useful information.

A quadtree meshing process has been implemented in order to substitute triangular meshing used in all the previous works reviewed. Flowfield reconstructions have been proven to be more accurate and smooth with quadtree meshes than the triangular ones. Tests have been carried on with Euler subsonic flowfields computed on two unstructured meshes with different wake refinement. Results show that Maskell integral is effectively corrected for planes located more than seven chords downstream showing little variations among the wake, allowing to evaluate drag for complex configurations, independently of their geometry.

## REFERENCES


[1] D Hue and S Esquieu. Computational drag prediction of the DPW4 configuration using the far-field approach. *Journal of aircraft*, **48**(5):1658–1670, 2011.

[2] D L Hunt, R M Cummings, and M B Giles. Wake integration for three-dimensional flowfield computations: Applications. *Journal of aircraft*, **36**(2):366–373, 1999.

[3] J Van der Vooren and J W Sloof. CFD-Based Drag Prediction: State-of-the-Art, Theory, Prospects. *National Aerospace Lab*, (TP 90247), 1990.

[4] D Destarac. Far-field Drag Extraction from Hybrid Grid Computations. *AAIA DPW-2*, 2003.

[5] K Kusunose. Drag prediction based on a wake-integral method. *AIAA paper*, **98-2723**:501–514, 1998.

[6] M B Giles and R M Cummings. Wake integration for three-dimensional flowfield computations: theoretical development. *Journal of aircraft*, **36**(2):357–365, 1999.

[7] C P Van Dam. Recent experience with different methods of drag prediction. *Progress in Aerospace Sciences*, **35**:751–798, 1999.

[8] Maskell E. C. Progress towards a method for the measurement of the components of the drag of a wing of finite span. *RAE Technical Report*, 1972.

[9] S Monsch, R Figliola, E Thompson, and J Camberos. Computation of Induced Drag for 3D Wing with Volume Integral (Trefftz Plane) Technique. *45th AIAA Aerospace Sciences Meeting*, **2007-1079**:1–9, 2007.

[10] R Löhner. Finite element methods in CFD: Grid generation, adaptivity, and parallelization. *AGARD-R-787*, 1992.

[11] D E Knuth. *The art of computer programming, volume 3.* Sorting and Searching. Addison Wesley Longman Publishing Co. Inc., 2 edition, 1998.

[12] W Yamazaki, K Matsushima, and K Nakahashi. Aerodynamic shape optimization based on drag decomposition. *24th AIAA Applied Aerodynamics Conference*, **2006-3332**:1–16, 2006.

[13] M Cordero-Gracia, M Gómez, J Ponsin, and E Valero. An interpolation tool for aerodynamic mesh deformation problems based on octree decomposition. *Aerospace Science and Technology*, **23**:93–107, 2011.